ISSN 1063-7826, Semiconductors, 2024, Vol. 58, No. 4, pp. 368–374. © Pleiades Publishing, Ltd., 2024.
Russian Text © The Author(s), 2023, published in Fizika i Tekhnika Poluprovodnikov, 2023, Vol. 57, No. 6, pp. 399–405.
English Text © Ioffe Institute, 2023.

Fabrication and Study of the Properties of GaAs Layers Doped with Bismuth

D. A. Zdoroveyshchev[a,*], O. V. Vikhrova[a], Yu. A. Danilov[a], V. P. Lesnikov[a], A. V. Nezhdanov[a], A. E. Parafin[b], and S. M. Plankina[a]

[a] *Lobachevsky State University, Nizhny Novgorod, 603022 Russia*

[b] *Institute for Physics of Microstructures, Russian Academy of Sciences, Nizhny Novgorod, 603950 Russia*

**e-mail: daniel.zdorov@gmail.com*

Received August 24, 2023; revised September 1, 2023; accepted September 1, 2023

Abstract—Pulsed laser deposition in vacuum at 220°C of GaAs layers heavily doped with Mn and/or Bi has been used to form nanostructures on *i*-GaAs (100) substrates. It is shown that, for the electrical activation of manganese, it is expedient to use subsequent annealing with an excimer laser pulse with a wavelength of 248 nm and a duration of 30 ns. The structures show an anomalous Hall effect with a hysteresis loop on the magnetic field dependence up to a Curie temperature of about ~70 K. Negative magnetoresistance is observed up to temperatures of ≈150 K. Bismuth does not prevent the activation of Mn atoms during annealing and contributes to an increase in the coercive field of the GaMnAs ferromagnetic semiconductor.

Keywords: gallium arsenide, pulsed laser deposition, Bi and Mn doping, pulsed laser annealing, ferromagnetic properties

DOI: 10.1134/S1063782624040171

1. INTRODUCTION

Bi atoms (element of group V of the Periodic Table) are isovalent for arsenic atoms and when they enter in the crystal lattice of gallium arsenide, they replace As with the development of a solid solution of the type $GaAs_{1-x}Bi_x$. Since Bi atoms are heavier than As atoms (209 and 75 a.m.u., respectively), a number of phenomena occur when they dope gallium arsenide.

Firstly, the width of the band gap (E_g) of the material decreases. It is shown in [1] that the value of E_g monotonically decreases from 1.42 eV (measurement temperature 300 K) for GaAs to 0.8 eV for GaAs with Bi content ~11 at %.

Secondly, the spin-orbit splitting energy increases noticeably (Δ_{SO}) in GaAs :Bi, even with small concentrations of bismuth. An increase in the value of Δ_{SO} from 0.34 eV (for GaAs) to ≈0.46 eV was observed in [2] with bismuth content ~1.8 at %.

Thirdly, Bi atoms have a specific effect on the transport of charge carriers in GaAs. Thus, [3] shows that the mobility of electrons changes insignificantly at concentrations of bismuth up to 1.6 at % in the layers of GaAs:Bi, while the mobility of holes decreases by an order of magnitude. Also, a drop of carrier concentration for *p*-type $GaAs_{1-x}Bi_x$ was observed [3] in addition to the decrease of mobility, which was explained by the authors by the appearance of bismuth clusters in GaAs, accompanied by the formation of trap states for holes.

Localization of holes in GaAs:Bi has been the subject of a number of theoretical and experimental studies (see, for example, [4]). In this regard, it should be noted that the question of the limit equilibrium solubility of Bi remains open. Thus, a conclusion is made about the low solubility of Bi in GaAs in [5], based on the theoretical calculation. However, the article [6] indicates the introduction of up to 20% bismuth into a solid solution $GaAs_{1-x}Bi_x$ during molecular beam epitaxy.

Segregation effects were observed when bismuth doped GaAs-based structures (see, for example, [6, 7]). The role of bismuth as a surfactant in the formation of structures with InAs quantum dots on the GaAs surface was noted in [8]. The authors believed that in the process of gas-phase epitaxy, the role of bismuth is to limit the migration mobility of other atoms on the surface of the growing layer, resulting in more homogeneous arrays of quantum dots.

In practical terms, bismuth doping may be important for increasing spin-orbit interaction in GaAs-based ferromagnetic semiconductor layers created by introducing several atomic percent transition elements (Mn) and having significant prospects for the manufacture of non-volatile memory devices, spin transfer structures and other spin-tronics devices [9].

It should be noted that in recent works, bismuth doping of GaAs-based structures is carried out, as a rule, in the process of molecular beam epitaxy (previously during liquid-phase and gas-phase epitaxy). However, molecular beam epitaxy facilities are very expensive, besides, each process requires a lot of time, which makes the method unsuitable even for small-scale production of device structures. Therefore, alternative, more productive and less economically costly GaAs doping methods are of interest. For example, ion implantation can listed among them, as well as the method of pulsed laser deposition used in this study for doping GaAs with bismuth in the process of growing layers. The joint doping of gallium arsenide with bismuth and a magnetic impurity (Mn) may also be important here for the development of spintronics materials.

2. EXPERIMENT PROCEDURE

Epi-ready semi-insulating GaAs plates with a surface orientation (100) were used as substrates for applying gallium arsenide layers doped with bismuth. The method of pulsed laser deposition (PLD) in vacuum was used in this study to form the structures GaAs:Bi and GaMnAs:Bi. This method is implemented in a chamber inside which a vacuum is created with a pressure of $\leq 10^{-6}$ Torr. The radiation of an Nd:YAG laser of the LQ-529 model, operating at the second harmonic with a wavelength of 532 nm, was introduced into the vacuum chamber through a quartz window, directed by an optical system to a rotating composite target (an undoped GaAs plate with a sector of metallic Mn and/or Bi) and sprayed it. The laser beam was focused on the target in a spot with an area of ~1.2 mm^2, and the energy density in the sputtering pulse was ~20 J/cm^2 (pulse energy ≈240 mJ) with a pulse duration of 10 ns and a repetition rate of ~10 Hz. The laser beam is displaced relative to the center of rotation of the target, so the trace of laser evaporation has the shape of a circle. The technological composition of the obtained layers was determined by the angle of the metal sector (Bi, Mn) inserted into this circle. A heated substrate holder is installed at a distance of ≈5 cm from the target. The process temperature for all manufactured structures was 220°C. The GaAs deposition rate measured using the TalySurf CCI 2000 (IPM RAS) device was ~2.0 ± 0.2 nm/min.

Our choice of the temperature for obtaining doped layers is due to the following circumstances. It was previously found in [10] that the phase composition is determined both by the amount of manganese introduced and by the temperature of the process during pulsed laser deposition of GaMnAs layers. In particular, at a technological manganese content of 17% in GaAs and a deposition temperature of 300°C, the formation of ferromagnetic clusters MnAs [10] was noted. The desire to minimize the probability of the formation of clusters of the second phase is due to a decrease in the application temperature to 220°C. It should be noted that GaMnAs layers are also usually formed by molecular beam epitaxy at temperatures close to temperatures used by us [11, 12].

Due to some specific characteristics of the PLD method (mainly due to the effect of laser plasma components on the growing layer), the formed GaAs with strong doping of Mn and/or Bi has a high electrical resistance, therefore an additional processing of structures grown at low temperature is needed. Thermal annealing cannot be used due to the formation in GaAs even at temperatures ~580°C of the second phase (MnAs in the case of manganese doping [12]) due to the low solid solubility of these impurities. An alternative is the nonequilibrium pulsed laser annealing method, which ensures the formation of single-phase layers of highly doped GaAs regardless of the method of preliminary introduction of the impurity (for example, Mn): by ion implantation [13] or PLD [10].

A number of samples in this study were subjected to post-growth pulsed laser annealing (PLA) using an LPX-200 excimer laser (KrF working mixture, wavelength 248 nm, pulse duration 30 ns). The sample was irradiated with a single defocused pulse with an area of ~1–1.5 cm^2. The pulse energy density ranged from 300 to 400 mJ/cm^2. The compositions of the samples, the parameters of application and annealing are listed in the following table.

The obtained structures were used to measure the sheet resistance and the Hall effect in van der Pauw geometry at room temperature using the Nanometrics 9500 system to determine electric transport characteristics and assess the impact of laser annealing on them.

The magnetic field dependences of the Hall resistance, as well as the magnetoresistance, which characterizes the spin-dependent scattering of charge carriers in magnetic semiconductors, were measured on structures with layers doped with manganese and bismuth in the temperature range of 6–300 K. These measurements were performed using a measuring system based on a closed-cycle helium cryostat Janis CCS-300S/202, including an electromagnet and a Keithley 2400 device that performs the functions of a current source and a voltage meter with an input resistance >10 GΩ.

Raman scattering (RS) spectra were studied using NTEGRA Spectra system manufactured by NT-MDT using 473 nm laser. The radiation was focused by a 100× lens with an aperture of NA = 0.9. The laser radiation power was 0.5 μW. The RS spectra were studied in the geometry of backscattering in the range 50–900 cm^{-1} with a resolution of 0.7 cm^{-1}. All spectra were obtained at room temperature.

3. EXPERIMENTAL RESULTS

The results of measurements of electrical properties by the Hall effect method at room temperature (sheet resistance R_S, layer concentration $n_s(p_s)$ and effective mobility of current carriers μ_H) are shown in Table 1. Structures with GaAs:Bi and GaMnAs:Bi layers obtained by the PLD method have an electronic type of conductivity and a sufficiently high layer resistance. It should be noted that the sheet resistance of the used initial substrate *i*-GaAs was $(3–5) \times 10^9$ Ω/□ (corresponds to the resistivity of the material ≈10^8 Ω cm), and electron mobility ≈3700–4800 cm^2/(V s). Thus, the resistance of structures with GaAs:Bi and GaMnAs:Bi layers is one and two orders of magnitude, respectively, less than the layer resistance of the original substrate *i*-GaAs; therefore, the shunting action of the substrate can be neglected in the first approximation.

Undoped GaAs layers grown by the PLD method under similar conditions (application temperature ≈250°C) have layer resistance ~3×10^9 Ω/□ and sufficiently high electron mobility (2600 cm^2/(V s)).

The Bi-1 and Bi-2 structures also show a layer resistance of >10^8 Ω/□ and *n*-type of conductivity after laser annealing, which corresponds to the absence of electrical activation of bismuth atoms. Drastic changes occurred after laser annealing of structures with layers doped with manganese. As a result PLA of the MnBi-1 and MnBi-2 structures, their layer resistance decreased to $R_S \approx 500$ Ω/□, the conductivity became hole, and the layer concentration of holes exceeded 10^{15} cm^{-2}, which indicates the electrical activation of manganese (acceptor) in the annealing process. The concentration increases with an increase in the energy density in the pulse and the mobility of the holes decreases (see the table). The mobility of holes (3–5 cm^2/(V s)) in MnBi-2 and MnBi-1 samples is characteristic of scattering on phonons and on ionized impurity in strongly doped GaAs (with concentration >10^{20} cm^{-3}) by acceptors [14]. The volume concentration of ionized acceptors of the MnBi-2 sample at the thickness of the doped layer ≈40 nm is estimated at ≈10^{21} cm^{-3}.

Next, we will consider the results obtained using Raman scattering spectroscopy. Figure 1 shows the RS spectra of structures before and after pulsed laser annealing. Only a peak attributable to LO-phonons and slightly (by ≈0.7 cm^{-1}) shifted to the "red" region from the value for undoped GaAs is observed on the spectrum obtained for the non-annealed Bi-0 structure (Fig. 1a) [15]. The RS spectrum (denoted as Bi-1) changes as a result of laser annealing with an energy density of 300 mJ/cm^2. The LO peak becomes higher and narrows from 4.6 cm^{-1} (the full width of the peak at half-height) for the initial sample up to 3.2 cm^{-1} for annealed sample. A peak corresponding to the GaAs TO-mode is also visible and is present in the spectrum

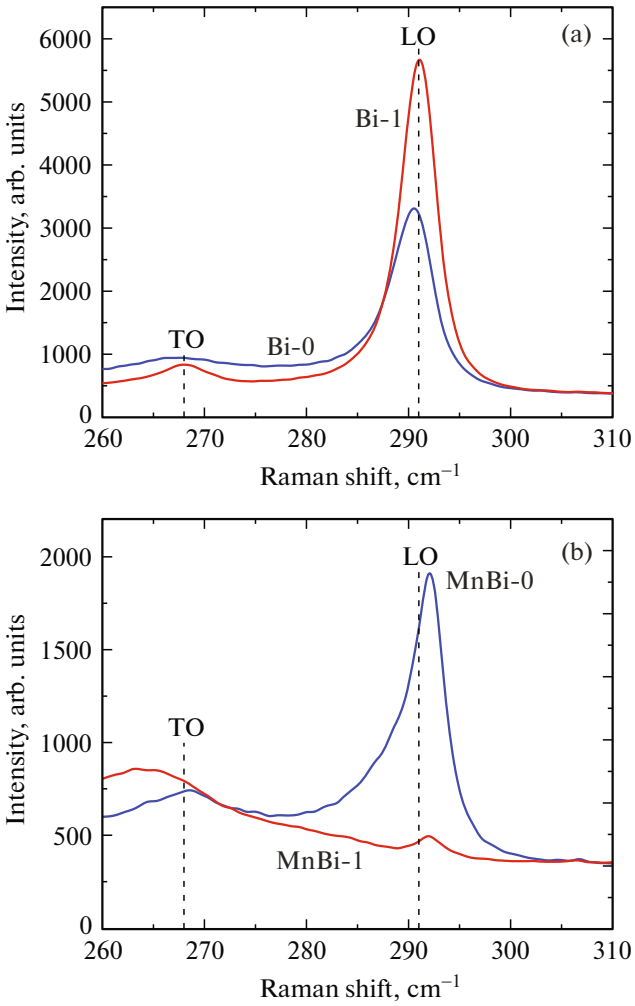

Fig. 1. Raman scattering spectra of laser grown and annealed (pulse energy density 300 mJ/cm^2) samples: (a) GaAs:Bi; (b) GaMnAs:Bi. The vertical dotted lines show the positions of peaks associated with TO- and LO-phonons in undoped GaAs [15]. (A color version of the figure is provided in the online version of the paper.)

due to disordering and/or a slight deviation from the backscattering geometry. At the same time, the frequencies of both peaks are close to the "literary" values for GaAs (291 and 268 cm^{-1} for LO- and TO-peaks, respectively) [15].

Figure 1b shows the RS spectra for samples with GaMnAs:Bi layers before and after PLA. Before laser annealing the spectrum consists of a LO peak shifted to the "blue" side by 0.9 cm^{-1} relative to the peak for GaAs and having a width of 3.2 cm^{-1}, and a low-intensity wide TO peak, also shifted to "blue" area by 0.8 cm^{-1} with respect to GaAs. The RS spectrum changed significantly after laser annealing: the intensity of the LO peak decreased significantly, although its position remained shifted. A wide band appeared at ≈265 cm^{-1}, which, taking into account the data of [16], should be interpreted as a coupled phonon-plas-

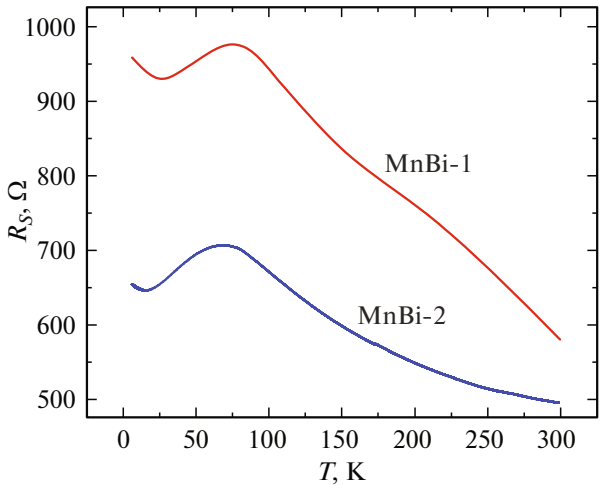

Fig. 2. Temperature dependences of the sheet resistance of GaMnAs:Bi samples after laser annealing with a pulse energy density of 300 and 400 mJ/cm^2.

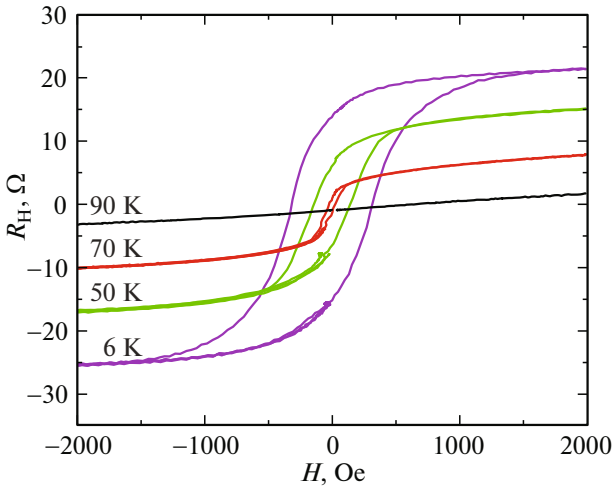

Fig. 3. Magnetic field dependences of the Hall effect at different measurement temperatures of the GaMnAs:Bi layer after laser annealing with a pulse energy density of 400 mJ/cm^2 (MnBi-2 sample).

mon mode (CPPM). The RS spectrum (not shown) of the MnBi-2 sample (laser annealing at an energy density of 400 mJ/cm^2) has the same features as the RS spectrum of the MnBi-1 sample, only the intensity of the CPPM band is noticeably higher.

Wide weak bands near 185 and 214 cm^{-1} are observed on all samples (this range is not shown in the graphs), which a number of authors interpret as GaBi-like TO- and LO-modes [17]. Other authors associate these bands with bismuth in the interstice and in the position of gallium (Bi_{Ga}) [18]. The intensity of these bands decreases in the Raman spectra after annealing.

A series of low-temperature measurements of the galvanomagnetic properties of layers of MnBi-1 and MnBi-2 structures was performed. Figure 2 shows the temperature dependences of the sheet resistance. Both dependences have a specific feature characteristic of ferromagnetic semiconductors and manifested in the occurrence of a peak on the temperature dependence of the resistance at a certain temperature, which is usually interpreted as the Curie temperature (the point of phase transition from the ferromagnetic state to the paramagnetic). MnBi-1 structure has maximum resistance at a temperature of 75 K and MnBi-2 structure has maximum resistance at ≈70 K.

Figure 3 shows magnetic field dependences of the Hall resistance (R_H) for the MnBi-2 sample with temperature variation. The Hall effect has a pronounced anomalous character. Note the presence of a hysteresis loop at temperatures up to 70 K. The width of the hysteresis loop (coercive field) monotonically decreases with an increase in the measurement temperature from 320 Oe at 6 K to ≈20 E at 70 K. The weak nonlinearity of the dependence Rh on the magnetic field strength in the absence of a hysteresis loop persists at higher temperatures (90 K). The magnetic field dependences of the Hall effect for the MnBi-1 sample (laser annealing at E = 300 mJ/cm^2) also have an anomalous appearance with a hysteresis loop up to a temperature of 75 K, despite the fact that the hysteresis loop is much narrower than for the sample MnBi-2. So, the coercive field is ≈135 Oe at 6 K and it monotonically decreases to 15 Oe at 70 K.

Magnetoresistance of MnBi-1 and MnBi-2 structures is negative at low temperatures. A specific feature of the magnetic field dependences of magnetoresistance is the preservation of a negative character at temperatures above the Curie temperature. Figure 4

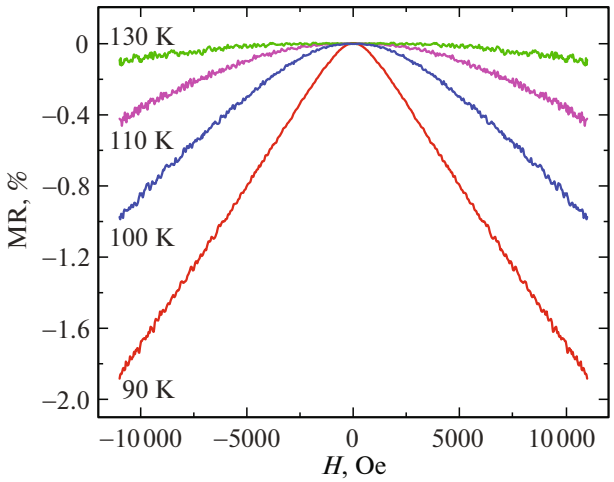

Fig. 4. Magnetoresistance at different temperatures for the GaMnAs:Bi layer after laser annealing with a pulse energy density of 300 mJ/cm^2 (MnBi-1 sample).

Table 1. Description of technological conditions for obtaining samples by pulsed laser deposition and electrical parameters of the initial structures, as well as structures subjected to pulsed laser annealing

Number structures	Process conditions		Electrical parameters of the layers			
	evaluation contents impurities, %	laser anneahng, E, mJ/cm^2	type conductivity	R_S, Ω/□	$n(p)_s$, cm^{-2}	μn, cm^2/(V s)
Bi-0	12 (Bi)	Without anneahng	n	5.2×10^8	2.05×10^7	580
Bi-1		300	n	1.8×10^8	2.5×10^8	140
Bi-2		400	n	4.4×10^8	3.0×10^7	470
MnBi-0	22 (Mn) and 6 (Bi)	Without anneahng	n	1.5×10^7	3.9×10^{10}	11
MnBi-1		300	p	580	2.05×10^{15}	5.3
MnBi-2		400	p	500	3.95×10^{15}	3.2

The thickness of the layers was ~40 nm.

shows the results of measuring the magnetoresistance of the MnBi-1 structure in the temperature range >90 K. It can be seen that a weak negative magnetoresistance occurs even at 130 K. A similar behavior was observed in case of the MnBi-2 structure.

4. DISCUSSION OF RESULTS

Firstly the attention is paid to the temperature of obtaining dopeded layers when discussing the results obtained. It is stated above that the temperature of the application process of 220°C was chosen to prevent the formation of MnAs-type clusters when obtaining GaMnAs layers. It is obvious, however, that this temperature does not allow avoiding point defects that occur in the growing layer when it is exposed to the laser plasma components. Residual defects (for example, the type of anti-structural defect As_{Ga}) may cause n-type of conductivity in the obtained layers. It is clear that the acceptor behavior of manganese atoms is not manifested in GaMnAs:Bi due to the presence of such defects (MnBi-0 sample in Table 1).

Annealing by pulse of excimer KrF laser with $E > 230$ mJ/cm^2 was successfully used in [19] for electrical activation of manganese in GaMnAs layers. Therefore, the "low-temperature laser deposition plus pulsed laser annealing" scheme is used in this work for forming layers doped with manganese and bismuth.

The results provided in the table show that this scheme works successfully in the case of joint doping of GaAs layers with manganese and bismuth: annealed GaMnAs:Bi layers have p-type of conductivity and a high layer concentration of holes ($>10^{15}$ cm^{-2}) even at the PLA energy density of 300 mJ/cm^2. The concentration of holes increases almost 2 times with an increase of E to 400 mJ/cm^2, and the mobility decreases, which indicates further embedding of manganese atoms in the gallium sublattice.

The presented results of electrical measurements are consistent with the data obtained by RS spectroscopy. The occurrence of a wide band at ≈265 cm^{-1} after PLA with $E = 300$ mJ/cm^2 and its interpretation as a bound phonon-plasmon mode is confirmed by electrical measurements: the volume concentration of holes recalculated from the layer value for the doped layer of the MnBi-1 sample is $\approx 5 \times 10^{20}$ cm^{-3} (this value is close to the value indicated in the work [16] for CPPM at 265 cm^{-1} the hole concentration value 7×10^{20} cm^{-3}). The increase of band intensity recorded by us at 265 cm^{-1} as a result of annealing with $E =$ 400 mJ/cm^2 correlates with a 2-fold increase of the concentration of holes in the doped Mn and Bi layer.

Studies of the RS spectra (comparison of peak widths in Figs. 1a and 1b) showed that bismuth doping does not disturb the GaAs crystal lattice as much as manganese doping. No CPPM is observed on the obtained RS spectra of GaAs:Bi layers, and a comparison of the spectra shows that the real content of bismuth introduced during laser deposition is lower than the technological one and is apparently <1.5%.

It can be stated that the introduction of bismuth atoms at PLD does not significantly (according to the RS data) disturb the GaAs structure and at least does not interfere with the electrical activation of manganese during laser annealing. The question of what is the real (different from technological) content of bismuth atoms introduced at PLD in the GaAs lattice is of interest and requires further research involving methods of elemental analysis.

The heating of the GaAs doped layer by a nanosecond excimer laser pulse allows a significant fraction of the introduced Mn atoms to occupy a replacement position in the gallium sublattice, thereby leading to the appearance of a high concentration of holes. The ferromagnetic exchange between manganese ions in the sites most likely occurs employs the mechanism of indirect exchange of the Ruderman–Kittel–Kasui-

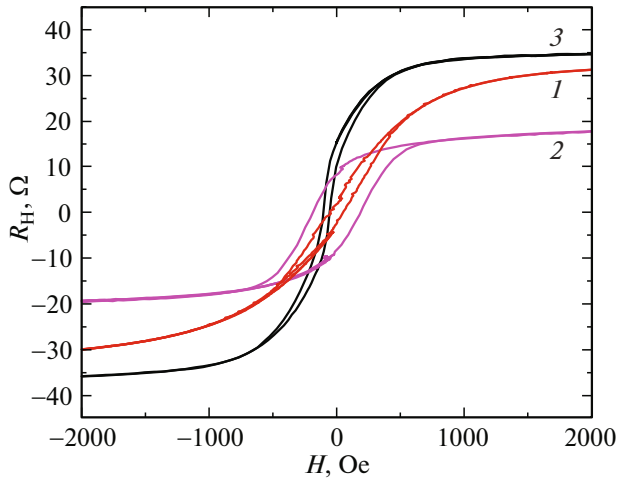

Fig. 5. Magnetic field dependences of the Hall effect at 40K for GaMnAs:Bi (curve *1*—MnBi-1 sample, curve *2*—MnBi-2 sample) in comparison with the GaMnAs layer [19] (curve *3*).

Yoshida type. The Curie temperature (~75 K) of the studied samples is quite typical for GaMnAs layers.

The negative magnetoresistance above the Curie temperature up to 150 K is due to paramagnetism associated with the presence of Mn ion magnetic moments and their alignment by an external magnetic field, as a result of which a decrease in the scattering of holes on magnetic scattering centers is observed. The depolarizing effect of thermal vibrations increases with an increase of the measurement temperature to 130–150 K and the effect of negative magnetoresistance disappears.

The question arises about the role of Bi atoms in the GaMnAs:Bi layers. Figure 5 shows a comparison of the magnetic field dependences of the Hall effect for the samples obtained in this work with a similar sample of the structure with a GaMnAs layer obtained using PLD method in the work [19]. It can be seen that the coercive field of a ferromagnetic semiconductor increased after the addition of bismuth, which qualitatively coincides with the data obtained for the GaMnAs:Bi structure grown using low-temperature molecular beam epitaxy method [20].

5. CONCLUSIONS

Thus, the paper demonstrates the fundamental possibility of doping GaAs layers with bismuth atoms in the process of pulsed laser deposition, as well as the joint introduction of Bi and Mn atoms into the growing layer. Measurements of Raman scattering of light and electrical properties showed that bismuth does not interfere with the electrical activation of Mn atoms during pulsed laser annealing. The Curie temperature of the obtained layers (70–75 K) slightly depends on the energy density of the laser pulse (300 or 400 mJ/cm^2). An anomalous Hall effect with a hysteresis loop is observed at low temperatures. The introduction of bismuth increases the coercive field of a ferromagnetic semiconductor. The results of determining the Curie temperature by the maximum temperature dependence of the layer resistance and by the decrease to zero of the coercive field coincide well. The effect of negative magnetoresistance in structures with GaMnAs:Bi layers occurs up to 150 K.

FUNDING

The study was sponsored by the Russian Scientific Foundation (grant no. 23-29-00312).

CONFLICT OF INTEREST

The authors of this work declare that they have no conflicts of interest.

REFERENCES

1. A. R. Mohmad, F. Bastiman, C. J. Hunter, R. D. Richards, S. J. Sweeney, J. S. Ng, J. P. R. David, B. Y. Majlis. Phys. Status Solidi B, **251**, 1276 (2014).
2. B. Fluegel, S. Francoeur, A. Mascarenhas, S. Tixier, E. C. Young, T. Tiedje. Phys. Rev. Lett., **97**, 067205 (2006).
3. R. N. Kini, A. Mascarenhas. In: *Bismuth-Containing Compounds* (Springer Series in Materials Science), **186**, 181 (2013).
4. K. Alberi, B. Fluegel, D. A. Beaton, M. Steger, S. A. Crooker, A. Mascarenhas. Phys. Rev. Mater., **2**, 114603 (2018).
5. N. Elayech, H. Fitouri, Y. Essouda, A. Rebey, B. El Jani. Phys. Status Solidi C, **20**, 138 (2015).
6. J. Sadowski, A. Kaleta, S. Kryvyi, D. Janaszko, B. Kurowska, M. Bilska, T. Wojciechowski, J. Z. Domagala, A. M. Sanchez, S. Kret. Sci. Rep., **12**, 6007 (2022).
7. J. Veletas, T. Hepp, K. Volz, S. Chatterjee. J. Appl. Phys., **126**, 135705 (2019).
8. B. N. Zvonkov, I. A. Karpovich, N. V. Baidus, D. O. Filatov, S. V. Morozov. FTP, **35** (1), 92 (2001). (in Russian).
9. T. Andrearczyk, K. Levchenko, J. Sadowski, K. Gas, A. Avdonin, J. Wrobel, T. Figielski, M. Sawicki, T. Wosinski. Materials, **16**, 788 (2023).
10. O. V. Vikhrova, Yu. A. Danilov, D. A. Zdoroveishchev, I. L. Kalentyeva, A. V. Kudrin, V. P. Lesnikov, A. V. Nejdanov, A. E. Parafin. FTT, **65** (5), 754 (2023). (in Russian).
11. T. Dietl, H. Ohno. Rev. Mod. Phys., **86**, 187 (2014).
12. H. Akinaga, J. De Boeck, G. Borghs, S. Miyanishi, A. Asamitsu, W. Van Roy, Y. Tomioka, L. H. Kuo. Appl. Phys. Lett., **72**, 3368 (1998).
13. S. Zhou. J. Phys. D: Appl. Phys., **48**, 263001 (2015).

14. J. S. Blakemore. J. Appl. Phys., **53**, R123 (1982).
15. K. Wan, J. F. Young. Phys. Rev. B, **41** (15), 10772 (1990).
16. W. Limmer, M. Glunk, S. Mascheck, A. Koeder, D. Klarer, W. Schoch, K. Thonke, R. Sauer, A. Waag. Phys. Rev. B, **66**, 205209 (2002).
17. J. A. Steele, R. A. Lewis, M. Henini, O. M. Lemine, D. Fan, Yu. I. Mazur, V. G. Dorogan, P. C. Grant, S.-Q. Yu, G. J. Salamo. Opt. Express, **22** (10), 11680 (2014).
18. M. J. Seong, S. Francoeur, S. Yoon, A. Mascarenhas, S. Tixier, M. Adamcyk, T. Tiedje. Superlattices Microstruct., **37** (11), 394 (2005).
19. O. V. Vikhrova, Yu. A. Danilov, B. N. Calls, A. V. Zdoroveishchev, A. V. Kudrin, V. P. Lesnikov, A. V. Nejdanov, S. A. Pavlov, A. E. Parafin, I. Yu. Pashenkin, S. M. Plankina. FTT, **59** (11), 2130 (2017).
20. T. Andrearczyk, K. Levchenko, J. Sadowski, J. Z. Domagala, A. Kaleta, P. Dluzewski, J. Wrobel, T. Figielski, T. Wosinski. Materials, **13**, 5507 (2020).

Translated by A. Akhtyamov